Capacity of Underwater Acoustic OFDM Cellular Networks

Balakrishnan Srinivasan, and Volkan Rodoplu
Department of Electrical and Computer Engineering
University of California, Santa Barbara, CA 93106-9560

Abstract—**We analyze the capacity of underwater acoustic cellular networks that utilize Orthogonal Frequency Division Multiplexing (OFDM) modulation. The capacity analysis is presented based on a model of the average path loss and frequency-dependent absorption, both of which are distance-dependent. We show that capacity-achieving systems utilize multiple architectural layers, each of which uses a different subband with its own frequency reuse number. We solve the problems of data rate maximization per mobile user, and the transmit power minimization under an average target data rate constraint per cell, for both the single- and multiple-layer architectural solutions. We discuss the practical issues in the implementation of such capacity-achieving underwater acoustic OFDM cellular systems.**

Index Terms—**underwater, cellular, acoustic, OFDM, multi-carrier, capacity**

I. Introduction

ONE of the fundamental problems in underwater networks is the delivery of sufficient data rates to underwater vehicles such as autonomous underwater vehicles (AUVs). Orthogonal Frequency Division Multiplexing (OFDM) is proving to be a promising technology for underwater acoustic communications, as shown by much of the recent physical-layer work [5][6][7]. The purpose of this paper is to evaluate the capacity of underwater acoustic OFDM *cellular* systems. Underwater acoustic cellular networks were pioneered in [1][2], where a capacity analysis of such systems that utilize single-carrier modulation was presented based on signal-to-interference (SIR) thresholds. The first contribution of this paper is to present the capacity analysis of underwater acoustic *OFDM* (multi-carrier) cellular systems, which can outperform single carrier modulation schemes by a large margin.

An important difference between the design of underwater acoustic cellular systems and the RF terrestrial cellular systems is the fact that underwater propagation shows a frequency-dependent absorption [3] in addition to distance-dependent path loss. The result of this in [1] for the single-carrier cellular system design was that the radius of a cell in the underwater cellular system is dependent on the frequency-reuse factor, whereas no such dependence exists for terrestrial cellular architectures.

The second contribution of this paper is the exploitation of this frequency-dependent absorption: We build multiple architectural layers in the cellular system, based on the principle that the higher frequencies, which show higher attenuation, should be repeated more frequently over the deployment region, and the lower frequencies should be repeated less frequently. In contrast with this idea, in [1], the cellular architecture was designed based on the choice of a single reuse factor N. We shall show that if the design uses multiple architectural layers each of which uses a different reuse number, the performance of the system can be improved by choosing the partition of the bandwidth between the different architectural layers optimally.

In this paper, we focus on OFDM systems. OFDM as a promising physical layer technology was investigated recently in [5]-[15]. In contrast with these techniques which are for point-to-point links, the aim of this paper is a system-level capacity analysis of underwater OFDM networks. This first analysis of the entire cellular network necessarily takes a more simplified model of the OFDM channel model. The analysis presented in this paper focuses on the effects of path loss and frequency-dependent absorption without modeling the effects of the Doppler shift and carrier synchronization, which we plan to address in our future work. Hence, the results in this paper are applicable to slowly-moving AUVs through the cellular network and can be taken as a performance upper bound for faster moving vehicles that will experience deterioration of the physical link due to the Doppler shift.

The channel in terrestrial cellular systems is also frequency-selective. However, the main difference here in an underwater acoustic channel is that the absorption increases monotonically as a function of the frequency. This monotonic dependence has the potential to lead to a multi-layered structure. In contrast, in a terrestrial system, the frequency dependence is much more random, and hence cannot be used to create architectural layers. As a result, one cannot go beyond physical layer techniques to combat frequency selectivity of terrestrial cellular systems. In contrast, in underwater acoustic networks, we can deal with the monotonic component of the frequency-selective channel at the network layer as we show in this paper. The remaining random component of the frequency-selective channel can still be combatted via the physical layer techniques in the literature.

The main difference between this paper and the physical layer OFDM techniques for acoustic communications in the literature is that we solve the system-level problems of (1) Optimal allocation of the OFDM subcarriers to different cells in the multi-layered cellular architecture, (2) Optimal power allocation on the set of subcarriers per cluster in the cellular architecture. The system-level design that we present is based

978-1-4244-5222-4/10/$26.00 ©2010 IEEE

on the *average* path loss and frequency-dependent absorption. Hence, this provides a coarse, system-level design. Given the optimal allocation that we derive in this paper, the physical layer OFDM techniques in the literature can then be applied, at a finer level, over the set of subcarriers that have been assigned to a particular base station.

We derive the capacity of underwater acoustic OFDM systems for the following two separate problems: (1) Maximization of the data rate per user, and (2) Minimization of the total transmit power per base station. The first problem is relevant to the bandwidth-limited regime of network operation where the main objective is to transfer the maximum data rate to each user. This is similar to the objectives pursued also in terrestrial cellular systems. The second objective is relevant to the energy-limited regime of network operation: In this regime, the amount of data to be transmitted to each user is small. Hence, we first fix the average data rate that we would like to deliver to each user. Given this, we minimize the total transmit power expanded by the base station. If the underwater base stations are battery-powered (which might be preferable over underwater cables), then conserving their power increases the lifetime of the cellular architecture itself. Hence, this decreases the frequency with which the batteries in the underwater base stations need to be replaced.

The rest of this paper is organized as follows: In Section II, we describe our system model and assumptions. In Section III, we formulate and solve the problem of finding the maximum data rate per cell in the interference-dominated regime, for both single and multiple architectural layers. In Section IV, we formulate and solve the minimum power problem, again for single and multiple architectural layers. In Section V, we present our simulation results. In Section VI, we discuss the related work in the literature, and we present our conclusions in Section VII.

II. System Model

In this section, we describe our system model. Our goal is to deploy a cellular architecture underwater, based on acoustic communication links, such that a regular hexagonal tessellation is employed. Because each base station, made up of transceivers, processors and packaging, is costly, we take an exogenous parameter μ to be the maximum allowed "base station density". In reality, typically, an area is under consideration for deployment, and a maximum number of base stations can be afforded to be deployed. In that setting, μ is found by dividing the number of base stations that can be afforded by the total area for deployment in question. The reason we choose to use the density μ rather than the particular number of base stations in our formulation, is to allow the design to be applicable to different sizes of deployment regions.

We assume that we are given a fixed bandwidth $[f_{min}, f_{min} + B]$ for the entire system, where f_{min} is the lowest edge frequency of the band, and B is the total bandwidth of the system (in Hertz). Each base station can have multiple transceivers, each of which possibly operates on a different part of the band. We assume that each base station uses OFDM, and that the width of a subcarrier Δf has been fixed for the entire system, such that the channel over each Δf in the band B is approximately flat. Then, this choice of Δf allows us to work with a discretized system, where we label the subcarriers from 1 to U, and let the ith subcarrier operate over $[f_{min} + (i-1)\Delta f, f_{min} + i\Delta f]$. We let SIR_i denote the signal-to-interference ratio of the i^{th} subcarrier; hence, SIR_i is found by integrating the received signal power over the subcarrier's band, and dividing it by the total interference over the same band. We present the analysis for the downlink in this paper. We assume that all of the base stations that utilize the same subcarrier transmit with the same average transmit power level, P_i, on that subcarrier. Further, we assume that the transmit signal distribution is Gaussian (hence, its variance is P_i). This assumption is used to be able to derive an analytical expression for the system capacity. We assume that the effect of the channel is to attenuate the transmit signal both by path loss and by frequency-dependent attenuation. Note that the effects of multipath interference, and Doppler shift are not modeled in this paper. The received signal is a scaled version of the transmitted signal, and hence, both the received signal and the received interference are Gaussian. In addition, note that our assumptions allow P_i to be different from P_j, when $i \neq j$.

Each architectural layer j in our system can be visualized as a separate cellular system, with its own reuse number N_j and its own cell radius R_j. Each layer will operate over its own subband B_j of the total bandwidth B, with no overlap between the bands used by different layers. The only requirement is that a base station must be deployed to the cell center of each architectural layer. Hence, the base station locations of the architectural layers must coincide on the plane. The following definition formalizes the concept of a multi-layered cellular system:

Definition 1 (Multi-layered cellular system) *A multi-layered cellular system* $S = (R, \{N_j\}, \{B_j\};$ $\mu, [f_{min}, f_{min} + B])$ *is defined as a cellular system that operates over the frequency band* $[f_{min}, f_{min} + B]$*, with a base station at the center of each cell in a regular tessellation. The radius* R *is the same for all of the cells, and* μ *is the maximum number of base stations that can be deployed per square meter. The system has multiple reuse numbers* $\{N_j\}$*. Each cellular system in this architecture that uses the particular reuse number* N_j *and the band* B_j *is called the "architectural layer"* j*.* $B_j \cap B_i = \emptyset$ *if* $i \neq j$*; that is, the bands used by different architectural layers are disjoint. Further,* $\cup_j B_j = [f_{min}, f_{min} + B]$*.* $R, \{N_j\}, \{B_j\}$ *are variables to be optimized, and* μ, f_{min}, B *are fixed parameters.*

A more general definition might have allowed the different architectural layers to possibly use different cell radii. However, the most efficient use of base stations is made when the cell centers of the different layers coincide to the extent possible. Hence, the above definition allows the layers to be built based on different reuse numbers $\{N_j\}$ rather than

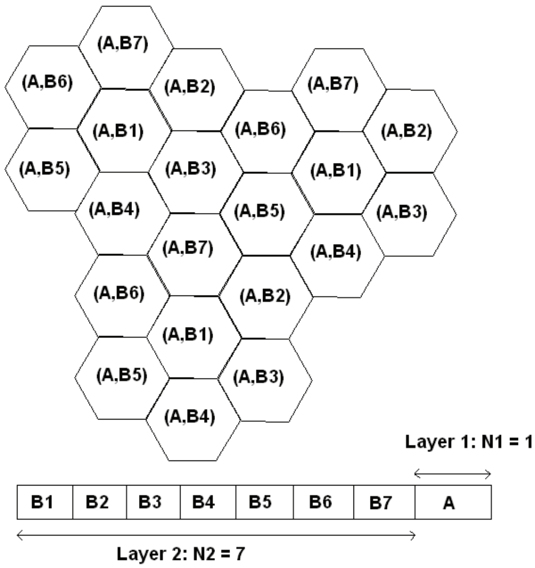

Fig. 1. Example system with two architectural layers

different cell radii.

An example of such a system is shown in Fig. 1. In this system, there are two architectural layers: $N_1 = 1$, and $N_2 = 7$, and each layer uses the same cell radius $R_1 = R_2 = R$. The bandwidth B is partitioned as shown in the figure. The partition in this example is by no means optimal because this partition gives an equal amount of bandwidth *(in Hertz)* to each cell. However, more fundamentally, a design should give the same *data rate* to each cell. In the next section, we address the problem of the maximization of data rate per cell, which will translate into the maximum data rate per user for a uniform user density.

III. Maximization of Data Rate per User

In this section, our aim is to derive the optimal number of layers, and the optimal partition of the bandwidth B to each layer and to each cell, such that the data rate per user is maximized. We assume that the user density, which we denote by ρ, is uniform throughout the deployment region. Then, maximizing the total data rate that each cell can deliver also maximizes the data rate per user. We divide this section into two subsections: First, we derive the optimal reuse number N^*, when only a single architectural layer is used. This illustrates the design procedure for this simple example. In the second subsection, we show how to design the multi-layered system.

A. Data Rate Maximization with a Single Architectural Layer

In a single-layer system, we need to determine only the optimal values of a common radius R^* for all cells, and the optimal reuse number N^*.

The total data rate that can be delivered over the U subcarriers is

$$R_{total} = \Delta f \sum_{i=1}^{U} log_2(1 + SIR_i) \tag{1}$$

Let d_0, k and $a(f)$ denote the reference distance, spreading factor and absorption coefficient respectively. Let $N_0(f_i)$ be the noise power spectral density as given in [3]. Then, the signal-to-interference-plus-noise ratio at each subcarrier i, denoted by $SINR_i$, is given by

$$SINR(f_i) = \frac{P_i (R/d_0)^{-k} (a(f_i))^{-R/d_0} \Delta f}{6P_i \sqrt{3N}^{-k} (R/d_0)^{-k} (a(f_i))^{-\sqrt{3N}R/d_0} \Delta f + N_0(f_i)\Delta f} \tag{2}$$

In the interference-limited regime, the P_i's are high, and the signal-to-interference ratio at subcarrier i, denoted by SIR_i, is the relevant quantity:

$$SIR(f_i) = \frac{P_i (R/d_0)^{-k} (a(f_i))^{-R/d_0} \Delta f}{6P_i \sqrt{3N}^{-k} (R/d_0)^{-k} (a(f_i))^{-\sqrt{3N}R/d_0} \Delta f} \tag{3}$$

Note that because each base station uses the same transmit power P_i on subcarrier i, these cancel out. Then, we define

$$K_N^{(i)}(R) \stackrel{\text{def}}{=} SIR(f_i) = \frac{(R/d_0)^{-k} (a(f_i))^{-R/d_0}}{6\sqrt{3N}^{-k} (R/d_0)^{-k} (a(f_i))^{-\sqrt{3N}R/d_0}} \tag{4}$$

This quantity is simply the channel gain divided by the sum of the channel gains of the interference. Then, we define

$$\tilde{R}_N^{(i)}(R) \stackrel{\text{def}}{=} \Delta f \; log_2(1 + K_N^{(i)}(R)) \tag{5}$$

This quantity is the contribution of the i^{th} subcarrier to the total data rate. Its dependence on the parameters R and N are explicitly shown via these indices. Then, the total data rate that a base station in cell c can deliver is

$$\tilde{R}(c) = \Delta f \sum_{i \in \tilde{B}(c)} log_2(1 + K_N^{(i)}(R)) \tag{6}$$

where $\tilde{B}(c) \stackrel{\text{def}}{=} \{i \mid c^{th} \text{ cell uses the } i^{th} \text{ subcarrier}\}$.

Now, our aim is to maximize the minimum data rate per square meter in any cell subject to the constraint that the base station density does not exceed μ. Let $\mathcal{C}$ denote the set of all cells. Then, our mathematical program is

Max-Rate, Single-Layer Program:

$$\max_{N,R} \frac{\tilde{R}_{min}}{\alpha R^2} \tag{7}$$

subject to

1) $\forall \; c \in \mathcal{C}$

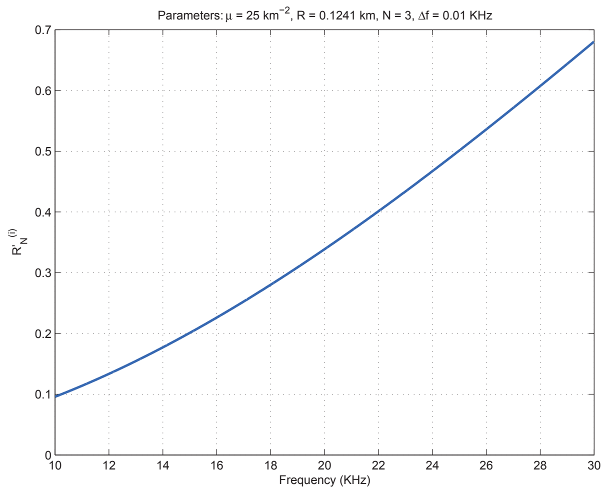

Fig. 2. Plot of $\tilde{R}_N^{(i)}(R)$ for $N = 3$

$$\sum_{i \in \tilde{B}(c)} \tilde{R}_N^{(i)}(R) \geq \tilde{R}_{min} \tag{8}$$

2) The number of base stations per unit area is less than or equal to μ.

Above, R and N are variables of the optimization program, and α is a constant whose value depends on the cell geometry. (For example, if the cells are hexagonal, $\alpha = 3\sqrt{3}/2$.)

Solution Method:

We solve this nonlinear optimization program by exploiting its special structure. We first exploit the symmetry of the regular tessellation (which extends over the entire 2-D plane), and note that in an optimal solution, the total data rate allocated to each cell should be the same. Hence, we define

$$\begin{aligned} \tilde{R}_{target}^{(N)}(R) &\stackrel{\text{def}}{=} \Delta f \ \frac{1}{N} \sum_{c=1}^{N} \sum_{i \in \tilde{B}(c)} log_2(1 + K_N^{(i)}(R)) \\ &= \Delta f \ \frac{1}{N} \sum_{i=1}^{U} log_2(1 + K_N^{(i)}(R)) \end{aligned} \tag{9}$$

as the target data rate that we would like to achieve in each cell. In this definition, the inside summation sums the contribution to the data rate of each subcarrier i that the cell c uses, and the outside summation sums over all the cells in the cluster of N cells, where N is the reuse number. This is divided by N, since this is the data rate that we want to give to each cell in that cluster. The equality after the definition expresses the same as a summation over all of the U subcarriers, and divides by N to find the data rate per cell in a cluster of N cells.

It can be seen that maximizing $ASE \stackrel{\text{def}}{=} \frac{\tilde{R}_{target}^{(N)}(R)}{\alpha R^2}$ over (N, R) maximizes the objective function of our optimization program. We shall carry this out in two steps. First, we fix N. Now, note that due to the functional dependence of $K_N^{(i)}(R)$ on R in (3), $ASE \sim \Theta(1/R)$. Hence, for each N, as R decreases, ASE increases. For any fixed N, the maximum ASE as a function of R is attained at $1/(\alpha R^{*2}) = \mu$. Hence, we fix the optimal radius for all architectural layers to $R^* = \sqrt{1/(\alpha\mu)}$. Having fixed R^*, we then maximize the ASE as a function of N.

We now describe the method to maximize over N, with R^* fixed. Fig. 2 shows the graph of a typical $\tilde{R}_N^{(i)}(R^*)$, for $N = 3$. Because the underlying function is continuous, and the Δf spacing very small, an equal amount of data rate can be allocated to each of the N cells in a cluster, by dividing the area under the curve in Fig. 2 into three roughly equal areas. The actual operation is to partition the set of subcarriers into subsets such that the sum of the data rate contributions of the subcarriers are equal. For this example, we partition the set of subcarriers such that

$$\sum_{c_1} log_2(1+K_N^{(i)}) \approx \sum_{c_2} log_2(1+K_N^{(i)}) \approx \sum_{c_3} log_2(1+K_N^{(i)}) \tag{10}$$

where c_1, c_2 and c_3 are the three cells in this cluster where $N = 3$. Because the underlying function is continuous, it is possible to partition the band into three subbands with equal areas under the function, as shown in the figure. In this choice, each cell uses a contiguous set of subcarriers. This choice is by no means unique; other, more complex, non-contiguous partitions that equalize the data rates over the cells are also possible. However, this partition allows the transceiver for each cell to be built more simply.

This partition produces $N^*(R^*)$, that is the optimal reuse number, for the fixed R^*. Hence, we have determined $N^* \stackrel{\text{def}}{=} \underset{N}{\text{argmax}} \frac{\tilde{R}_{target}^{(N)}(R^*)}{\alpha R^{*2}}$. The maximum data rate per user is given by $\frac{\tilde{R}_{target}^{(N^*)}(R^*)}{\rho \alpha R^2}$.

B. Data Rate Maximization with Multiple Architectural Layers

In a multi-layered system, we need to determine the optimal reuse numbers N_j and the corresponding bands B_j for the architectural layers. In order to do this, we need to solve the following optimization program:

Max-Rate, Multi-Layer Program:

$$\max_{N_1, N_2, \ldots, N_U, R} \frac{\tilde{R}_{min}}{\alpha R^2} \tag{11}$$

subject to

1) $\forall\ c \in \mathcal{C}$

$$\sum_{i \in \tilde{B}(c)} \tilde{R}_{N_i}^{(i)}(R) \geq \tilde{R}_{min} \tag{12}$$

2) The number of base stations per unit area is less than or equal to μ.

Solution Method:

The optimal value of the cell radius is the same for each

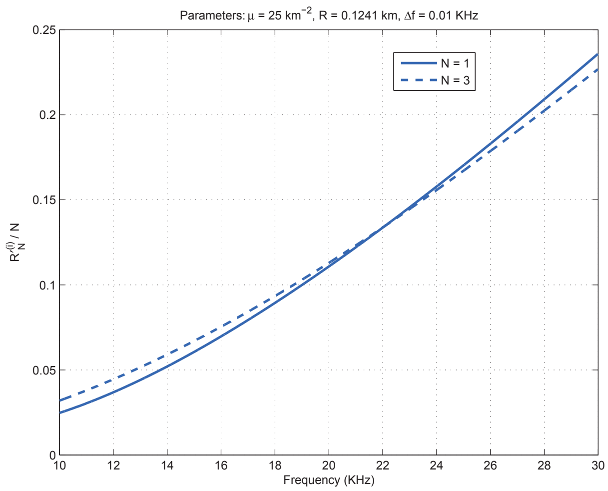

Fig. 3. Plot of $\tilde{R}_N^{(i)}(R)/N$ for $N=1$ and $N=3$

architectural layer and is set, for the same reason as in the previous subsection, to $R^* = \sqrt{1/(\mu\alpha)}$.

In the case of a multi-layered system, we utilize the frequency dependence of SIR to vary the reuse number across the band $[f_{min}, f_{min}+B]$. Specifically, for each subcarrier i, we determine the optimal reuse number that maximizes the data rate contribution per cell from that subcarrier, i.e., $N_i^* = \underset{N}{\operatorname{argmax}} \frac{\tilde{R}_N^{(i)}(R^*)}{N}$. Next, we collect the subcarriers for which the optimal reuse number is the same and thus form the bands B_j, i.e., $B_j = \{i \mid N_i^* = N_j\}$. Let the number of distinct N_j's thus obtained be denoted by J. This also represents the number of architectural layers for the system. Note that each base station in the system takes part in each of the J architectural layers, and has a separate set of transceivers dedicated to each architectural layer. The average data rate delivered by each base station in the j^{th} architectural layer is given by $\frac{1}{N_j}\sum_{i\in B_j}\tilde{R}_{N_j}^{(i)}(R^*)$. The maximum data rate per user for this multi-layered system is given by $\frac{1}{\rho\alpha R^{*2}}\sum_{j=1}^{J}\frac{1}{N_j}\sum_{i\in B_j}\tilde{R}_{N_j}^{(i)}(R^*)$. For each architectural layer j, the set of subcarriers $i \in B_j$ is partitioned into subsets, as explained in the previous subsection, such that the sum of the data rate contributions of the subcarriers are equal.

The formation of multiple architectural layers is illustrated graphically in Fig. 3, in which we plot $\tilde{R}_N^{(i)}(R^*)/N$ for $N=1$ and $N=3$. In this case, there are two architectural layers and their corresponding bands are on either side of the point at which the curves intersect. The optimal $\tilde{R}_N^{(i)}(R^*)/N$ curve is the "upper envelope" of the curves. In Fig. 3, the architectural layer with $N=3$ will use the band from 10 KHz to 23 KHz, and the architectural layer with $N=1$ will use the band from 23 KHz to 30 KHz. Further, the band $[10,23]$ KHz will be divided into three subbands such that the data rates from each of the subbands are roughly equal.

IV. Minimization of Transmit Power per Base Station

In this section, we consider system design in the energy-limited regime, in which the amount of data to be transmitted is small and the focus is on minimizing the transmit power of the base stations. We assume that the noise power in the subband corresponding to each subcarrier is comparable to the interference power in that subband. Again, as in Section III, we assume that the user density ρ is uniform throughout the deployment region. Since a large cell size would mean more transmit power for the base stations (compared to a smaller cell size), we seek to use the minimum possible value for the cell radius. Hence, we fix the cell radius to $R=\sqrt{1/(\mu\alpha)}$. Our aim is to minimize the average transmit power per base station subject to the constraint that a certain minimum data rate per user, or equivalently, data rate per unit area is guaranteed by the system. We divide this section into two subsections. In the first subsection, we consider design with a single architectural layer, in which we seek the optimal reuse number, i.e., the reuse number for which the average transmit power per base station is minimum. In the second sub-section, we describe how the solution to the above problem leads to a design with multiple architectural layers.

A. Transmit Power Minimization with a Single Architectural Layer

In this subsection, we set up the optimization program to solve the problem of finding the optimal reuse number and the optimal transmit power allocation across the frequency band $[f_{min}, f_{min}+B]$, which is used by a single architectural layer.

The contribution of the i^{th} subcarrier to the total data rate is given by $\Delta f \ \log_2(1+SINR(f_i))$, where $SINR(f_i)$ is as defined in equation (2). The average data rate per unit area is given by

$$T(N,P_1,P_2,...,P_U) \stackrel{\text{def}}{=} \frac{\Delta f}{N\alpha R^2}\sum_{i=1}^{U}\log_2(1+SINR(f_i)) \quad (13)$$

The average transmit power per base station is given by $\frac{1}{N}\sum_{i=1}^{U}P_i$. Now, we want to determine the values of $N,P_1,P_2,...,P_U$ that would minimize the average transmit power per base station subject to the constraint that the average data rate per unit area is at least a minimum A. The optimization program is set up as follows:

Min-Power, Single-Layer Program:

$$\min \frac{1}{N}\sum_{i=1}^{U}P_i \quad (14)$$

over all $N,P_1,P_2,...,P_U$, subject to

1) $T(N,P_1,P_2,...,P_U) \geq A$
2) $P_i \geq 0$ for $i=1,2,...,U$.

Solution Method:

First, we note that for any fixed N, the function

$T(N, P_1, P_2, ..., P_U)$ is concave in the vector $\mathbf{P}$. Hence, for a fixed N, we have an optimization sub-program. The feasible set of the sub-program, when it is non-empty, is convex, and maximizes a linear function over this convex set. Hence, when the program is feasible, a global maximum of this sub-program exists, and can be found via any nonlinear optimization method (such as the SQP algorithm used by $fmincon$ function in MATLAB). Because the reuse factor N takes on discrete values from a limited set of cellular reuse factors (up to a practical maximum N_{max}), the optimal N^* is chosen as the N that has the minimum value of the objective function, over the set of optimal values obtained for the convex sub-programs.

After we determine the optimal reuse number N^*, we partition the set of subcarriers into N^* subsets with the optimal power level P_i^* for each subcarrier, such that the data rate contributions of the subcarriers are all equal to A. We shall illustrate this with examples in Section V.

B. Transmit Power Minimization with Multiple Architectural Layers

In this subsection, we set up the optimization program to derive the optimal number of architectural layers, and the corresponding reuse numbers N_j and the bands B_j for a multi-layered system. We let the reuse number be variable for the subbands corresponding to each subcarrier in the available frequency band. Let the reuse number for the subband corresponding to the i^{th} subcarrier be denoted by N_i.

The average data rate per unit area is given by

$$G(N_1, N_2, ..., N_U, P_1, P_2, ..., P_U) \stackrel{\text{def}}{=} \frac{\Delta f}{\alpha R^2} \sum_{i=1}^{U} \frac{1}{N_i} \log_2(1 + SINR(f_i)) \quad (15)$$

where $SINR(f_i)$ is as defined in equation (2). In this case, the average transmit power per base station is $\sum_{i=1}^{U} \frac{P_i}{N_i}$. Again, as in Section IV-A, we want to minimize the average transmit power per base station subject to the constraint that the average data rate per unit area is at least a minimum A. Now, the optimization program is:

Min-Power, Multi-Layer Program:

$$\min \sum_{i=1}^{U} \frac{P_i}{N_i} \quad (16)$$

over all $N_1, N_2, ..., N_U, P_1, P_2, ..., P_U$, subject to

1) $G(N_1, N_2, ..., N_U, P_1, P_2, ..., P_U) \geq A$
2) $P_i \geq 0$ for $i = 1, 2, ..., U$.

Solution Method:
First, we note that for any fixed vector of N_i's, which we denote by $\mathbf{N}$, the function $G(N_1, N_2, ..., N_U, P_1, P_2, ..., P_U)$ is concave in $\mathbf{P}$. Hence, the feasible set of this sub-program with a fixed $\mathbf{N}$ is convex. Because the sub-program maximizes a linear function on a convex feasible set, whenever the sub-program is feasible, a global minimum of the sub-program exists. The main difficulty here is that, even though each N_i takes on discrete, allowable values of reuse factors, the search space grows exponentially with U. We solve this problem by noting that with the particular $SINR_i$'s in our problem, the optimal $\mathbf{N}$ vector is a monotonically decreasing, step function of i. Hence, we search over this discrete, bounded space of the optimal solutions of the sub-programs, and pick the one that achieves the minimum.

The solution of the above program provides us the set of optimal reuse numbers N_i^*. As explained in Section III-B, we collect the subcarriers that have a common reuse number and form the bands B_j, where $B_j = \{i \mid N_i^* = N_j\}$. The number of unique N_j thus obtained, denoted by J, represents the number of architectural layers for the system.

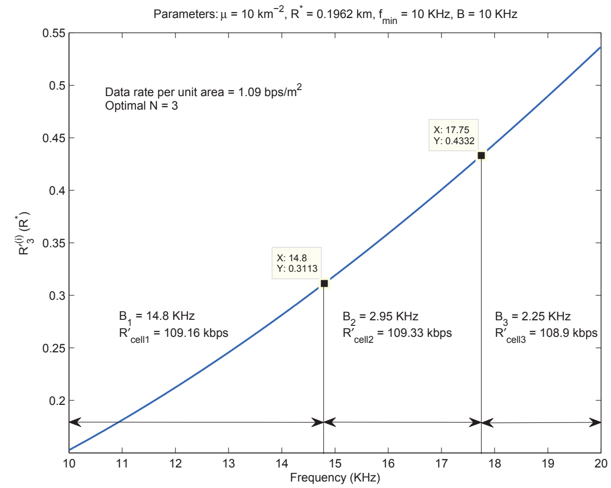

Fig. 4. Plot of $\tilde{R}_3^{(i)}(R^*)$ versus frequency and band partitions for $\mu = 10$

V. Simulation Results

In this section, we present our simulation results. We divide this section into two subsections. In the first subsection, we focus on the results obtained with the objective of maximizing the data rate per user. In the second sub-section, we analyze the results of the simulation for transmit power minimization. For the simulations in both the subsections, we use the following values for the different parameters: $d_0 = 10$ m, $\alpha = 3\sqrt{3}/2$ (hexagonal cell geometry), $k = 1.5$ and $\Delta f = 0.01$ KHz. We use the empirical formula given in [4] for the absorption coefficient $a(f)$. In order to be practical, we restrict the value of reuse number N to be no more than 39 in our simulations.

A. Maximum Data Rate Per User

First, we focus on the design with a single architectural layer. We illustrate an example with $f_{min} = 10$ KHz, $B = 10$ KHz and $\mu = 10$ base stations per km^2. In this case, the cell radius is $R^* = 0.1962$ km. Since the cell radius is fixed, we evaluate the data rate per cell (given by (9)) for each N and determine the N for which the quantity is a maximum. For this example, we find that the optimal reuse number is $N = 3$ and the maximum data rate per cell is 109.13 kbps. In Fig. 4, we plot $\tilde{R}_3^{(i)}(R^*)$ against frequency and illustrate a

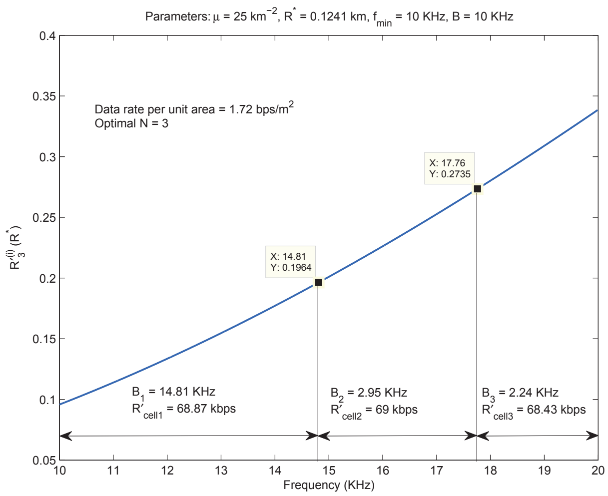

Fig. 5. Plot of $\tilde{R}_3^{(i)}(R^*)$ versus frequency and band partitions for $\mu = 25$

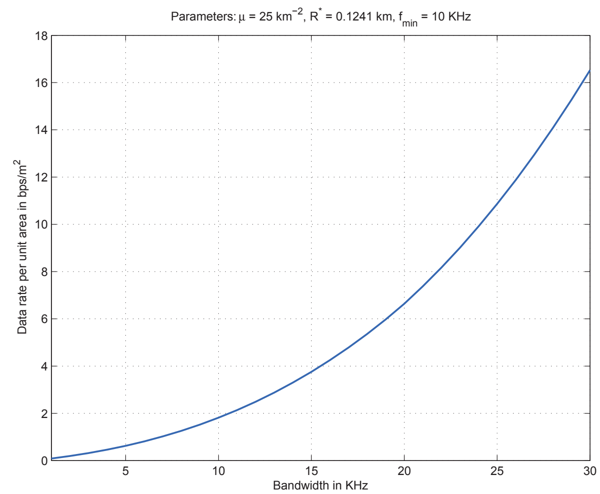

Fig. 6. Data rate per unit area versus bandwidth

partition of the set of subcarriers into three sets of subcarriers such that the data rate from each set is roughly equal to 109.13 kbps. With this particular partition, we observe that the number of subcarriers in each set is different and it decreases as the frequency increases. This behavior is expected because the SIR improves with frequency resulting in improved data rates at higher frequencies. In this example, the data rate per unit area is 1.09 bps/m^2. If the user density $\rho = 10$ users/km^2, then the data rate per user for this system is 109 kbps.

In order to demonstrate the effect of changing the value of the base station density μ, we consider the same example with $\mu = 25$ base stations per km^2. As a result, the cell radius is decreased to $R^* = 0.1241$ km. Again, we find that the optimal reuse number is $N = 3$. But the maximum data rate per cell is 68.77 kbps. Fig. 5 shows the plot of $\tilde{R}_3^{(i)}(R^*)$ against frequency and illustrates a partition of the set of subcarriers into three sets of subcarriers such that the data rate from each set is roughly equal to 68.77 kbps. We observe that the band partitions occur at nearly the same frequencies as for $\mu = 10$. In this example, the data rate per unit area is 1.72 bps/m^2. For a user density of $\rho = 10$ users/km^2, the data rate per user is 172 kbps. As we increase μ, the optimal cell radius R^* decreases, with the effect that the SIR (for the same reuse number N) is reduced. This results in reduced total data rate and reduced data rate per cell. However, the rate of decrease of the data rate is slower than the rate of decrease of the area of the cell (with increased base station density), and as a result, the data rate per unit area increases. For a given user density, the system is able to provide more data rate per user with more base stations per unit area.

We now consider the effect of bandwidth on the data rate per user. Fig. 6 shows the plot of maximum data rate per unit area against the bandwidth B available to the system for $f_{min} = 10$ KHz and $\mu = 25$ base stations per km^2. Since the total data rate increases with bandwidth, the data rate per unit area (and hence, data rate per user for a given user density) also increases with bandwidth. Fig. 7 illustrates that the optimal reuse number changes with bandwidth while the values of the other system parameters are being held constant. In this example, beyond $B = 20$ KHz, $N = 1$ turns out to be the optimal reuse number. In Fig. 8, we show the plot of maximum data rate per unit area obtained by varying the lower band edge frequency f_{min} for $B = 10$ KHz and $\mu = 25$ base stations per km^2. Since the SIR increases with frequency, the maximum total data rate and the data rate per user increase as f_{min} is increased and this trend is also evident from the plot. From Fig. 9, we observe that the optimal reuse number also changes with f_{min} (while the values of the other system parameters remain fixed). For $B = 10$ KHz, in this example, beyond $f_{min} = 15$ KHz, the optimal reuse number is $N = 1$.

Now, we consider the design with multiple architectural layers. To compare with the design of a single-layer system, we take the example considered earlier with $f_{min} = 10$ KHz, $B = 10$ KHz and $\mu = 10$ base stations per km^2. We determine the optimal reuse numbers and the corresponding bands for the architectural layers as outlined in section III-B. For this example, we obtain two architectural layers with reuse numbers $N_1 = 3$ and $N_2 = 1$ respectively. The corresponding bands are formed as shown in Fig. 10. In Fig. 10, we also illustrate the partitioning of subcarriers within the architectural layer with reuse number 3. The data rates per unit area in the two architectural layers are 0.635 bps/m^2 and 0.463 bps/m^2 respectively, and the overall data rate per unit area for the system is just the sum of these two quantities. For a user density of $\rho = 10$ $users/km^2$, the data rate per user is 109.75 kbps, which is higher than that obtained with the single-layer system designed using the same parameters.

We consider another example for a multi-layered system with $f_{min} = 1$ KHz, $B = 29$ KHz and $\mu = 25$ base stations per km^2. In this case, again, we obtain two architectural layers with $N_1 = 1$ and $N_2 = 3$. However, the band corresponding to reuse number N_1 consists of two non-contiguous sub-bands

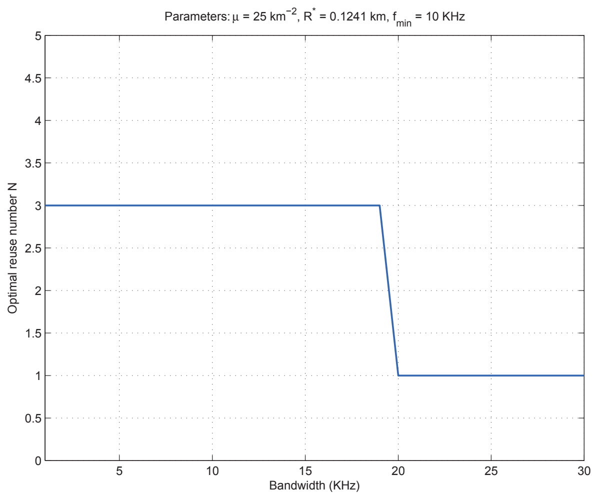

Fig. 7. Optimal reuse number versus bandwidth

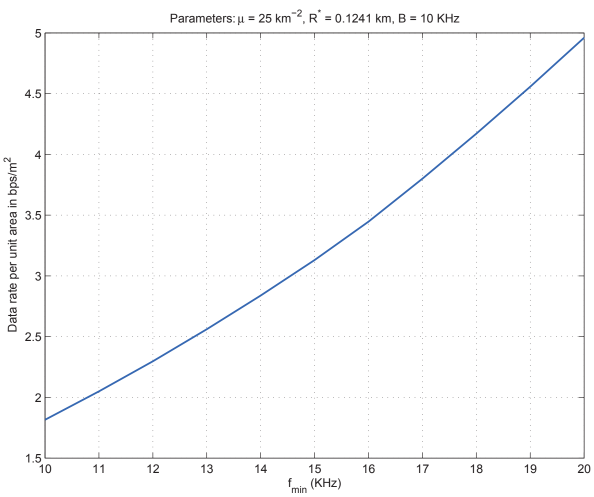

Fig. 8. Data rate per unit area versus f_{min}

as shown in Fig. 11. This corresponds to the intersection of the $\tilde{R}_N^{(i)}(R^*)/N$ curves (for $N = 1$ and $N = 3$) at two distinct points within the available frequency band. The data rates per unit area in the two architectural layers are 3.68 bps/m^2 and 2.65 bps/m^2 respectively, and for a user density of $\rho = 10$ $users/km^2$, the data rate per user is 632.37 kbps. As observed earlier, an increase in the available bandwidth has resulted in an increase in the data rate per user.

B. Minimum Transmit Power per Base Station

We now shift our attention to system design with a single architectural layer with the objective of minimizing the average transmit power per base station subject to the constraint that the system should provide a certain minimum data rate per unit area. In our simulations, we determine the solution of the optimization program set up in section IV-A, in two steps. We fix the reuse number N, and then determine the optimal transmit power allocation for this N. We repeat the process

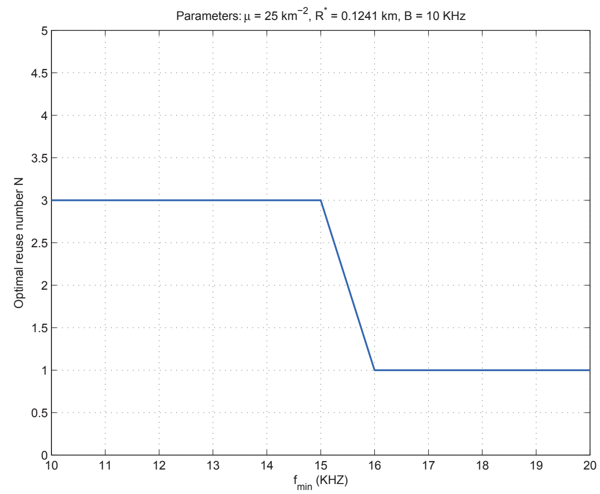

Fig. 9. Optimal reuse number versus f_{min}

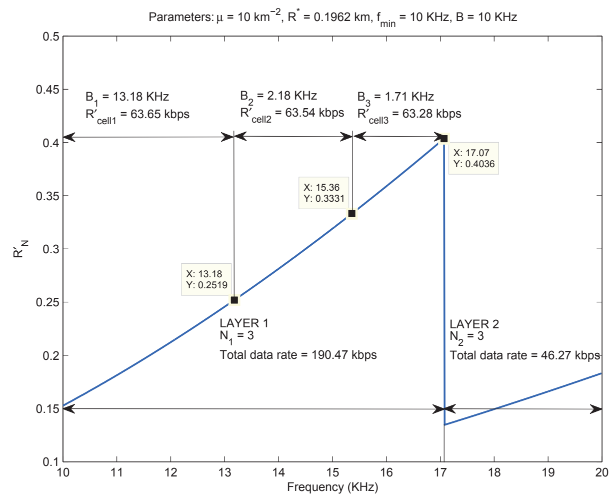

Fig. 10. Multiple architectural layers

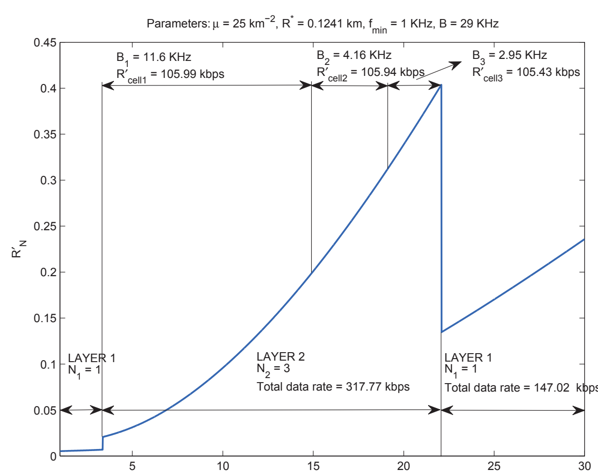

Fig. 11. Multiple architectural layers: non-contiguous bands for $N_1 = 1$

for each N, and determine the optimal value of N as the one for which the average transmit power per base station is a minimum.

We consider an example with $f_{min} = 10$ KHz, $B = 5$ KHz and $\mu = 25$ base stations per km^2. For a target data rate of 1 $kbps/km^2$, the optimal reuse number turns out to be $N = 1$. Fig. 12 shows the optimal transmit power allocation across the subcarriers in the band 10 KHz to 15 KHz, for the reuse numbers $1, 7, 13$ and 19. We observe that as N increases, the number of subcarriers for which a non-zero transmit power is allocated, increases. For example, in Fig. 12, for $N = 1$, only the subcarriers from 10 KHz to around 10.6 KHz carry a non-zero transmit power, whereas for $N = 19$, all subcarriers from 10 KHz to around 11.75 KHz are needed to meet the same target data rate constraint. When the target data rate per unit area is doubled, we find that, for each N, a higher number of subcarriers in the available frequency band are allocated a non-zero transmit power. The target data rate constraint also implies that each cell within any cluster should provide the same data rate to the user. As N increases, the cluster size increases, and the $SINR$ (for a given power level) also increases, thereby increasing the total data rate. However, the rate of increase of the total data rate with N is smaller than the rate of increase of the cluster size. This tends to decrease the data rate delivered per cell. Hence, in order to achieve the required data rate per unit area, a design with a higher reuse number needs to use more number of subcarriers and more transmit power for each subcarrier.

We now consider system design with multiple architectural layers with the objective of solving the minimum power problem. We solve the optimization program as outlined in Section IV-B. We expect that the higher frequency subcarriers will use a lower reuse number compared to the lower frequency subcarriers, and also that the reuse numbers that are more likely to reduce the average transmit power per base station are $N = 1$ and $N = 3$. We make use of this intuition to avoid the complexity of searching over all possible combinations of reuse numbers across the subbands (corresponding to each subcarrier), and search for the optimal solution among the solutions that use $N = 3$ for some of the subcarriers and $N = 1$ for the remaining set of subcarriers in the band. For the example considered in single layer design, with $f_{min} = 10$ KHz, $B = 5$ KHz, $\mu = 25$ base stations per km^{-2} and a target data rate of 1 $kbps/km^2$, we solve the optimization program with fixing $N = 3$ for the first subcarrier in the band and $N = 1$ for all the remaining subcarriers, and find the optimal power allocation across the subcarriers. By comparing the average transmit power with that of the single layer design with $N = 1$, we find that using $N = 1$ for all subcarriers is the optimal solution for this example.

We consider a second example with $f_{min} = 10$ KHz, $B = 5$ KHZ, $\mu = 25$ base stations per km^{-2} and a target data rate of 2 $kbps/km^2$. Even in this case, we find the average transmit power increases (compared to the case of single layer design with $N = 1$) when the combination of $N = 3$ for the first subcarrier in the band and $N = 1$ for all the remaining subcarriers is used. We note that the average transmit power would increase even further if $N = 3$ is used for more than one subcarrier. We also note that a reuse number greater than 3 for some of the subcarriers would tend to increase the average transmit power. Hence, we conclude that the optimal solution for this particular set of parameters is to use a single architectural layer with reuse number $N = 1$. However, we expect that for some set of the system parameter values and target data rate, a design with multiple architectural layers will outperform a design with a single architectural layer in terms of minimizing the average transmit power. In that case, we expect that there would be multiple subbands (corresponding to multiple architectural layers) and the subbands in the lower part of the available frequency band would use a higher reuse number and the subbands in the higher part of the available frequency band would use a lower reuse number.

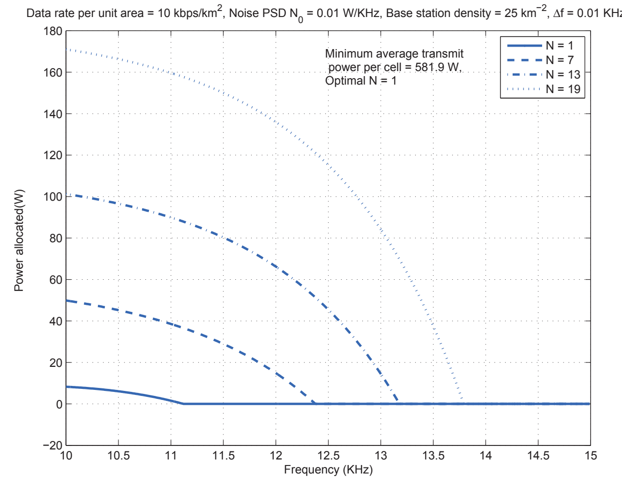

Fig. 12. Transmit power allocation: target data rate $= 1$ $kbps/km^2$

As a general conclusion, compared with the *single-carrier* underwater acoustic cellular system design in [1], which found a wide range of optimal reuse numbers, we see that the optimal design of underwater cellular OFDM networks use small reuse numbers such as 1 and 3, when multiple layers are allowed in the design. The reason is that the coefficient $(1/N_i)$ in front of the logarithmic data rate contribution of subcarrier i is too strong a penalty compared with the data rate increase obtained via the interference term inside the logarithm. As a result, optimal designs choose not to incur this penalty and retain small cluster sizes.

VI. Related Work

The related work can be divided roughly into two categories: Physical layer developments in underwater acoustic OFDM communications on point-to-point links, and the capacity analysis of OFDM systems. Physical layer techniques have focused on the development of OFDM low-complexity detectors [5][6][7], channel modeling [8][9], coded OFDM [10], MIMO-OFDM [11][12][13], synchronization [14], and hardware implementation [15]. The main challenges at the physical layer are carrier synchronization in the presence of Doppler shift, and timing acquisition of spread-spectrum signals, both of which exist for terrestrial RF systems as well but are exacerbated by the acoustic channel.

The Shannon capacity of terrestrial OFDM systems was investigated in [16][17][18] and [19]; however, the channel models did not model the distance-dependent path loss in these works. The capacity analysis of cellular terrestrial systems, which model the distance-dependent path loss as well as large-scale fading, is standard, and can be found in [20]. The first work to propose a cellular architecture for underwater networks, and to derive its capacity was [1]. The current paper essentially derives the capacity of such underwater acoustic networks under *multi-carrier* modulation.

For terrestrial cellular OFDM systems, several works in the literature have applied power allocation algorithms. In [21], the authors maximize the throughput of a multi-cell OFDM system under a power constraint; however, the reuse factor is fixed (and does not appear in this maximization). It is not on a per-cell basis; hence, does not maximize the area spectral efficiency of the design. Finally, the terrestrial systems do not show frequency-dependent absorption. In [22], the authors analyze the downlink capacity of an OFDM-based terrestrial cellular system. Even though the channel model has large-scale fading in addition to path loss, the results are for fixed frequency reuse numbers (only 1 and 3), and no capacity optimization framework is presented. In [23], the authors present algorithms for dynamic resource allocation in the downlink of multimedia systems that are based on OFDM; however, no cellular structure has been presumed. In [24], heuristics are presented to solve the subcarrier allocation and bit loading problems in OFDMA, and the formulation does not presume any cellular structure.

VII. Conclusions

In this paper, we analyzed the capacity of an underwater acoustic cellular network that uses OFDM modulation, under a system design that allows multiple architectural layers in a cellular system, such that each subcarrier can possibly use a different reuse number. We have found that optimal designs typically use small reuse numbers such as 1 and 3 in the multi-layer solutions. We described how to allocate the subcarriers optimally to the base stations such that the data rate is maximized, or the minimum power solution is attained.

References

[1] M. Stojanovic, "Frequency reuse underwater: capacity of an acoustic cellular network," in *Proc. ACM International Workshop on Underwater Networks (WUWNet'07)*, pp. 19-24, Sept. 2007.

[2] M. Stojanovic, "On the design of underwater acoustic cellular systems," in *Proc. IEEE OCEANS 2007-Europe*, pp. 1-6, June 2007.

[3] M. Stojanovic, "On the relationship between capacity and distance in an underwater acoustic communication channel," in *Proc. ACM International Workshop on Underwater Networks (WUWNet'06)*, pp. 41-47, Sept. 2006.

[4] L. Berkhovskikh and Y. Lysanov, *"Fundamentals of Ocean Acoustics,"* New York: Springer, 1982.

[5] A. K. Morozov, J. C. Preisig, "Underwater acoustic communications with multi-carrier modulation," in *Proc. IEEE OCEANS 2006*, pp. 1-6, Sep. 2006.

[6] M. Stojanovic, "Low complexity OFDM detector for underwater acoustic channels," in *Proc. IEEE OCEANS 2006*, pp. 1-6, Sep. 2006.

[7] J. Huang, J. Sun, C. He, X. Shen, A. Zhang, "High-speed underwater acoustic communication based on OFDM," in *Proc. IEEE MAPE 2005*, vol. 2, pp. 1135-1138, Aug. 2005.

[8] B-C. Kim, I-T. Lu, "Parameter study of OFDM underwater communication systems," in *Proc. IEEE OCEANS 2000*, vol. 2, pp. 1251-1255, Sep. 2000.

[9] Y. V. Zakharov, V. P. Kodanev, "Multipath-Doppler diversity of OFDM signals in an underwater acoustic channel," in *Proc. IEEE ICASSP 2000*, vol. 5, pp. 2941-2944, Jun. 2000.

[10] Z. Kun, Q. S. Sen, K. T. Aik, T. B. Aik, "A real-time coded OFDM acoustic modem in very shallow underwater communications," in *Proc. IEEE OCEANS 2006-Asia Pacific*, pp. 1-5, May 2007.

[11] R. F. Ormondroyd, "A robust underwater acoustic communmication system using OFDM-MIMO," in *Proc. IEEE OCEANS 2007-Europe*, pp. 1-6, Jun. 2007.

[12] B. Li, S. Zhou, M. Stojanovic, L. Freitag, J. Huang, P. Willett, "MIMO-OFDM over an underwater acoustic channel," in *Proc. IEEE OCEANS 2007*, pp. 1-6, Sep. 2007.

[13] Z. Xu, Y. V. Zakharov, V. P. Kodanev, "Space-time signal processing of OFDM signals in fast-varying underwater acoustic channel," in *Proc. IEEE OCEANS 2007-Europe*, pp. 1-6, Jun. 2007.

[14] W. Wei, X. Hu, D. Wang, R. Xu, H. Sun, "Performance comparison of time synchronization algorithms for OFDM underwater communication," in *IEEE M2VIP 2007*, pp. 104-107, Dec. 2007.

[15] N. Nasri, H. Ben, A. Kachouri, M. Abdellaoui, M. Samet, "Moduation/demodulation techniques with FPGA's architecture to improve OFDM wireless underwater communication transceiver," in *Proc. IEEE DTIS 2006*, pp. 400-403, 2006.

[16] H. Bolcskei, D. Gesbert, A. J. Paulraj, "On the capacity of OFDM-based spatial multiplexing systems," *IEEE Trans. Commun.*, vol. 50, issue 2, pp. 225-234, Feb. 2002.

[17] S. Ohno, G. B. Giannakis, "Capacity maximizing MMSE-optimal pilots for wireless OFDM over frequency-selective block Rayleigh-fading channels," *IEEE Trans. Info. Theory*, vol. 50, issue 9, pp. 2138-2145, Sep. 2004.

[18] M. Codreanu, M. Juntti, M. Latvo-Aho, "Low-complexity iterative algorithm for rinding the MIMO-OFDM broadcast channel sum capacity," *IEEE Trans. Commun.*, vol. 55, issue 1, pp. 48-53, Jan. 2007.

[19] R. Zhang, L. Ying-Chang, R. Narasimhan, J. M. Cioffi, "Approaching MIMO-OFDM capacity with per-antenna power and rate feedback," *IEEE Jour. Sel. Areas Commun.*, vol. 25, issue 7, pp. 1284-1297, Sep. 2007.

[20] T. Rappaport, *Wireless Communications: Principles and Practice*, 2nd Edition, Chapter 1, Prentice Hall, NJ, 2001.

[21] C-H. Yi, E. Geranotis, "Centralized power allocation algorithms for OFDM cellular networks," in *Proc. IEEE MILCOM 2003*, vol.2, pp. 1250-1255, Oct. 2003.

[22] C. Huo, A. B. Sesay, A. O. Fapojuwo, "Analysis of downlink capacity for an OFDM based cellular system,"in *Proc. IEEE MILCOM 2005*, vol.5, pp. 3219-3225, Oct. 2005.

[23] N. Damji, T. Le-Ngoc, "Dynamic downlink OFDM resource allocation with interference mitigation and macro diversity for multimedia services in wireless cellular systems," in *Proc. IEEE WCNC 2005*.

[24] G. Kulkarni, S. Adlakha, M. Srivastava, "Subcarrier allocation and bit loading algorithms for OFDMA-based wireless networks," *IEEE Trans. Mobile Computing*, vol. 4, no. 6, Nov./Dec. 2005.